

Communication

# The Function of Different Subunits of the Molecular Chaperone CCT in the Microsporidium *Nosema bombycis*: NbCCT $\zeta$ Interacts with NbCCT $\alpha$

Sheng Xu <sup>1,†</sup>, Ying Chen <sup>1,†</sup>, Jingru Qi <sup>1,†</sup>, Runpeng Wang <sup>1</sup>, Erjun Wei <sup>1</sup>, Qiang Wang <sup>1,2</sup>, Yiling Zhang <sup>1,2</sup>, Xudong Tang <sup>1,2</sup>  and Zhongyuan Shen <sup>1,2,\*</sup> 

<sup>1</sup> College of Biotechnology, Jiangsu University of Science and Technology, Zhenjiang 212100, China; xu18609659561@163.com (S.X.); 17853577156@163.com (Y.C.); jingru.qi@biortus.bio (J.Q.); qb1999517@126.com (R.W.); wejust@163.com (E.W.); wqiang523@126.com (Q.W.); zhangyiling008@126.com (Y.Z.); xudongt@just.edu.cn (X.T.)

<sup>2</sup> Sericulture Research Institute, Chinese Academy of Agricultural Sciences, Zhenjiang 212100, China

\* Correspondence: szysri@163.com

<sup>†</sup> These authors contributed equally to this work.

**Abstract:** Chaperonin containing tailless complex polypeptide 1 (CCT) is a molecular chaperone protein that consists of eight completely different subunits and assists in the folding of newly synthesized peptides. The zeta subunit of CCT is a regulatory factor for the folding and assembly of cytoskeletal proteins as individuals or complexes. In this study, the zeta subunit of *Nosema bombycis* (NbCCT $\zeta$ ) is identified for the first time. The complete ORF of the NbCCT $\zeta$  gene is 1533 bp in length and encodes a 510 amino acid polypeptide. IFA results indicate that NbCCT $\zeta$  is colocalized with actin and  $\beta$ -tubulin in the cytoplasm during the proliferative phase and that NbCCT $\zeta$  is completely colocalized with NbCCT $\alpha$  in the cytoplasm of *N. bombycis* throughout the entire life cycle. Furthermore, the yeast two-hybrid assay revealed that the NbCCT $\zeta$  interacts with NbCCT $\alpha$ . The transcriptional level of NbCCT $\zeta$  is significantly downregulated by knocking down the NbCCT $\alpha$  gene, while the transcriptional level of NbCCT $\alpha$  is downregulated after knocking down the NbCCT $\zeta$  gene. These results suggest that NbCCT $\zeta$  may play a vital role in the proliferation of *N. bombycis* by coordinating with NbCCT $\alpha$ .



**Citation:** Xu, S.; Chen, Y.; Qi, J.; Wang, R.; Wei, E.; Wang, Q.; Zhang, Y.; Tang, X.; Shen, Z. The Function of Different Subunits of the Molecular Chaperone CCT in the Microsporidium *Nosema bombycis*: NbCCT $\zeta$  Interacts with NbCCT $\alpha$ . *J. Fungi* **2024**, *10*, 229. <https://doi.org/10.3390/jof10030229>

Academic Editor: Matthew S. Sachs

Received: 29 January 2024

Revised: 15 March 2024

Accepted: 17 March 2024

Published: 20 March 2024



**Copyright:** © 2024 by the authors. Licensee MDPI, Basel, Switzerland. This article is an open access article distributed under the terms and conditions of the Creative Commons Attribution (CC BY) license (<https://creativecommons.org/licenses/by/4.0/>).

**Keywords:** microsporidia; chaperonin; CCT $\zeta$ ; coordinating function; immunolocalization

## 1. Introduction

Microsporidia are obligate intracellular parasites that are capable of infecting diverse vertebrates and invertebrates including humans [1]. So far, 220 genera and 1700 species of microsporidia have been identified [2]. *Nosema bombycis* is the pathogen causing pebrine disease in silkworms and is transmitted both horizontally and vertically to silkworms and leads to considerable economic losses in the sericulture industry [3].

The synthesis and folding of nascent peptides occur throughout the entire life cycle of microsporidia. The chaperonin-containing tailless complex polypeptide 1 (CCT), a molecular chaperone protein known as the T-complex 1, plays a crucial role in the correct folding of proteins [4]. Each loop of CCT has eight different subunits (CCT1–CCT8, also known as CCT $\alpha$ –CCT $\theta$ ) with three characteristic domains: the apical domain, the equatorial domain, and the intermediate domain. The apical domain comprises the loop that forms the lid, the equatorial domain encompasses the ATP binding site, and the intermediate domain contains the conserved aspartic acid essential for ATP hydrolysis [5–7]. A growing number of studies show that about 10–15% of newly synthesized proteins interact with CCT, including numerous essential structural and regulatory proteins such as the cell cycle regulator CDC20, the cancer-related VHL tumor suppressor, and WD40-repeat proteins [7–9]. Meanwhile, CCT is also involved in many fundamental cellular processes, including cell

division [10], metabolism, transcription and translation [11], cellular trafficking, and signal transduction [12].

The cellular functions of the eukaryotic CCT chaperone were first associated only with the folding of the cytoskeletal protein tubulin and actin [6]; however, the sequences of the substrate-binding domains at the top of the eight subunits differ remarkably, resulting in different types of substrate binding. Therefore, different subunits may have different functions as well [13,14]. CCT $\alpha$  is necessary for ciliate assembly and the maintenance of axial filament structure [15]. CCT $\beta$  and CCT $\delta$  bind to actin, while tubulin interacts with all CCTs [6]. CCT $\theta$  is associated with the migration of tumor cells, and ectopic expression leads to the high aggressiveness of esophageal squamous cell carcinoma (ESCC) [16,17], whereas CCT $\gamma$  inhibits the migration of cancer cells [18,19]. CCT $\zeta$  is a regulatory factor for cytoskeleton assembly and cell cycle regulation [20,21].

In this study, the NbCCT $\zeta$  (the CCT $\zeta$  of *N. bombycis*) was identified for the first time. NbCCT $\zeta$  is colocalized with Nb-actin and Nb $\beta$ -tubulin in the cytoplasm of proliferating *N. bombycis*. Moreover, NbCCT $\zeta$  interacts with NbCCT $\alpha$  and is colocalized with NbCCT $\alpha$ . The knockdown of NbCCT $\zeta$  resulted in the downregulated expression of the NbCCT $\alpha$  gene, while the expressional level of the NbCCT $\zeta$  gene was also affected by the knockdown of the NbCCT $\alpha$  gene. Our data suggest that the NbCCT $\zeta$  may play a vital role in the proliferation of *N. bombycis*.

## 2. Materials and Methods

### 2.1. Parasite and Host

The NbCCT $\alpha$  antibody, Nb $\beta$ -tubulin antibody, Nb-actin antibody, and *N. bombycis* were provided by the Sericultural Research Institute of the Chinese Academy of Agricultural Sciences.

### 2.2. Cloning and Bioinformatic Analysis of NbCCT $\zeta$

The purified spore suspension of *N. bombycis* ( $10^9$  spores/mL) was ground for 1 min with a bead grinder and then cooled on ice for 5 min, repeated 6 times. The genomic DNA was extracted with a fungal genomic DNA extraction kit and stored at  $-20\text{ }^\circ\text{C}$  following concentration measurement.

According to the partial sequences of NbCCT $\zeta$  on the NCBI database as well as the homologous sequences of the CCT $\zeta$  of other microsporidian species, the specific forward primer 5'-CCGGAGCTCATGCAATCCACTCAATCCGAC-3' and reverse primer 5'-CCCTCGAGTTATTGTTCAATCTTCTTCTTCTTA-3' were designed and synthesized (Sangon Biotech, Shanghai, China). PCR amplification was performed using the *N. bombycis* genomic DNA as a template comprising 25  $\mu\text{L}$  of PrimeSTAR HS DNA Polymerase (Takara Biotechnology, Dalian, China), 2  $\mu\text{L}$  per primer, 2  $\mu\text{L}$  of genomic DNA, and 19  $\mu\text{L}$  of ddH<sub>2</sub>O. The following parameters were applied in the amplification system: predenaturation at  $95\text{ }^\circ\text{C}$  for 5 min and PCR amplification at  $98\text{ }^\circ\text{C}$  for 10 s,  $55\text{ }^\circ\text{C}$  for 15 s, and  $72\text{ }^\circ\text{C}$  for 90 s, totaling 35 cycles. The amplified product was detected on 1% agarose gel and was purified using an Axyprep DNA gel extraction kit (AP-GX-4, Axygen Bioscience, Union City, CA, USA). Then, the product with polyA tail was ligated to the pMD19-T vector overnight at  $16\text{ }^\circ\text{C}$ . The pMD19-T-NbCCT $\zeta$  recombinant plasmid was transformed into the TOP10 competent cells. Positive clones were confirmed through blue-white screening, and the recombinant plasmids were sequenced by Sangon Biotech (Shanghai, China).

Multiple sequence alignment was performed by using DNAMAN8 software (DNAMAN8.0 for Windows). The isoelectric point and relative molecular mass of protein were predicted on Compute\_Pi/Mw ([https://web.expasy.org/compute\\_pi/](https://web.expasy.org/compute_pi/), accessed on 23 January 2023). The transmembrane domain was predicted with TMHMM Server v (<http://www.cbs.dtu.dk/services/TMHMM/>, accessed on 23 January 2023). N-glycosylation modification was predicted with NetNGlyc 1.0 (<http://www.cbs.dtu.dk/services/NetNGlyc/>, accessed on 23 January 2023). O-glycosylation was predicted with YinOYang 1.2 (<https://services.healthtech.dtu.dk/service.php?YinOYang-1.2>, accessed on 23 January 2023).

Phosphorylation was predicted by using NetPhos 3.1 (<https://services.healthtech.dtu.dk/service.php?NetPhos-3.1>, accessed on 24 January 2023). The signal peptide was predicted by SignalP5.0 (<http://www.cbs.dtu.dk/services/SignalP/>, accessed on 24 January 2023). The secondary structure was predicted on PSIPRED (<http://bioinf.cs.ucl.ac.uk/psipred/>, accessed on 24 January 2023). The subcellular localization of NbCCT $\zeta$  was predicted using Cell-PLoc2.0 (<http://www.csbio.sjtu.edu.cn/bioinf/Cell-PLoc-2/>, accessed on 24 January 2023).

### 2.3. Expression and Purification of NbCCT $\zeta$ Recombinant Protein

By analyzing the sequence of hydrophobicity, homology, antigenicity, hydrophilicity, and the possibility of protein expression in a prokaryotic system, the sequence region 168–390 with a length of 223 amino acids was selected for antibody preparation. The target sequence was amplified with the specific primers F-*Bam*H I (5'-TCAGGATCCGTTAAAGCTATAAAAAATATCTC-3') and R-*Xho* I (5'-GATCTCGAGTTTAAGAGAGGCTCTAAT-3'), and then the pET28a-NbCCT $\zeta$ -233 plasmid was generated by inserting the NbCCT $\zeta$ -233 gene into *Bam*H I and *Xho* I-digested pET28a plasmid. The NbCCT $\zeta$ -233 recombinant protein was expressed and purified according to a previous report [22].

### 2.4. Preparation of NbCCT $\zeta$ Polyclonal Antibody and Western Blot

The purified protein obtained above was used to prepare polyclonal antibodies. Briefly, New Zealand rabbits were immunized with equal amounts of recombinant protein and incomplete Freund's adjuvant every 15 days, and the serum was collected on the 53rd day. Polyclonal antibodies were obtained by using antigen affinity column purification, and the preimmune serum was collected as a negative control.

The total protein of *N. bombycis* was extracted by breaking the spores with acid-washed glass beads. NbCCT $\zeta$  was detected in the total protein of *N. bombycis* using the NbCCT $\zeta$  antibody.

### 2.5. Immunolocalization of NbCCT $\zeta$ in *N. bombycis*

Mature spores of *N. bombycis* were germinated in 0.1 M KOH at 27 °C for 0.5 h. The BmN cells were inoculated with the germinating spores in six-well plates. The colocalization of NbCCT $\zeta$  with Nb $\beta$ -tubulin, Nb-actin, or NbCCT $\alpha$  was investigated according to our previous work [23].

### 2.6. RNAi

Small interfering RNA (siRNA) was designed and synthesized by Sangong Biotech (Shanghai, China). Fresh mulberry leaves were coated with 10<sup>8</sup> spores/mL of microsporidia. The silkworm larvae of the fifth instar were fed on the above-obtained mulberry leaves. Following 6 h of feeding, 3  $\mu$ L of siRNA (Table 1) was injected into each larva. The midguts from three independent silkworm samples were collected at 24 h, 48 h, 72 h, and 96 h post-siRNA injection and stored at –80 °C.

The specimens were lysed with 1 mL of RNAiso plus lysate (9108Q, Takara, Dalian, China), and the total RNA was extracted with a Mini Best universal RNA extraction kit (9767, Takara Biotechnology, Dalian, China). cDNA was synthesized with a PrimeScript RT master mix (RR036B, Takara Biotechnology, Dalian, China) and was used as the template. RT-qPCR was performed by using the TB green premix Ex Taq II (Tli RNase H Plus) kit (RR820A, Takara Biotechnology, Dalian, China). The primer sequences are listed in Table 1. The transcriptional level was calculated by using the 2<sup>– $\Delta\Delta$ ct</sup> method with three replicates. The multiple *t*-test was conducted using GraphPad Prism 8.0 (GraphPad Software, San Diego, CA, USA).

**Table 1.** Primer sequences for RNAi and RT-qPCR.

Gene		Sequences
<i>NbCCTζ</i> (RNAi)	Sense	GCUAUUAGAGCCUCUCUUATT (5'-3')
	Antisense	UAAGAGAGGCUCUAAUAGCTT (5'-3')
Negative control (RNAi)	Sense	UUCUCCGAACGUGUCACGUTT (5'-3')
	Antisense	ACGUGACACGUUCGGAGAATT (5'-3')
<i>NbCCTζ</i> (RT-qPCR)	Forward	AGCCAGAGCTATTGCTGCTTTTGG (5'-3')
	Reverse	GAATACCAGCCTTGGCAAGGATTTC (5'-3')
<i>NbCCTα</i> (RT-qPCR)	Forward	GGTGGGGCTATTGAAGTCGC (5'-3')
	Reverse	CCAAACCCGCATTTATTGCCA (5'-3')
<i>BmGAPDH</i> (RT-qPCR)	Forward	TTCATGCCACAACCTGCTACA (5'-3')
	Reverse	AGTCAGCTTGCCATTAAGAG (5'-3')
<i>SSrRNA</i> (RT-qPCR)	Forward	TCGAGTGCCAGCAGCCGCGG (5'-3')
	Reverse	CGATCCTTAGCTTACGTCC (5'-3')

### 2.7. Yeast Two-Hybrid Assay

The *NbCCTα* gene was amplified using the genomic DNA of *N. bombycis* with specific primers (F-*EcoR* I: 5'-CATGGAGGCCGAATTCATGTTCAACGAAATCTCTACTAACA-3', R-*Not* I: 5'-GCTAGTTATGCGGCCTTATTTCTGTTTGGCATTATTATT-3'). The *NbCCTζ* gene was amplified using specific primers (F-*EcoR* I: 5'-GGAGGCCAGTGAATTCATGCAATC-CACTCAATCCGA-3', R-*Xho* I: 5'-TCATCTGCAGCTCGATTATTGTTCAATCTTCTTCTTCCTT-3'). The *NbCCTα* gene was ligated into the *EcoR* I and *Not* I-digested yeast two-hybrid bait vector pGBKT7-BK, whereas the *NbCCTζ* gene was ligated into *EcoR* I and *Xho* I-digested prey pGADT7-AD using an In-Fusion HD Cloning Kit (638909, Takara, Kusatsu, Japan), respectively. The bait recombinant vector and the prey recombinant vector were cotransformed into Y2H Gold yeast cells (YC1002, Weidi Biotech, Shanghai, China). The cotransformed cells were cultured on SD/-Leu/-Trp plates (630489, TaKaRa, Kusatsu, Japan) at 28 °C. The single colony on SD/-Leu/-Trp plates was chosen and cultured on SD/-Ade/-His/-Leu/-Trp/X-a-gal plates (630462, TaKaRa, Kusatsu, Japan) at 28 °C.

## 3. Results

### 3.1. Cloning and Expression of *NbCCTζ* and Western Blot

The complete nucleotide sequence of the *NbCCTζ* gene (NCBI accession number: PP069767.1) was obtained by PCR amplification and sequencing. The results showed that the ORF of the *NbCCTζ* gene was 1533 bp and that it encodes a polypeptide of 510 amino acids (Figure S1). The bioinformatic analysis showed that the predicted molecular weight is 57 kDa and that there is no signal peptide and no transmembrane domain. The prediction of phosphorylation sites and glycosylation sites indicated that the *NbCCTζ* may have 32 phosphorylation sites and 2 N-glycosylation sites. The secondary structure analysis showed that the *NbCCTζ* gene is mainly composed of helix and coil. Multiple sequence alignment indicated that *NbCCTζ* shares a certain degree of homology with that of other microsporidia, especially *Nosema granulosis* (79.80%) and *Vairimorpha ceranae* (62.28%), but has a low degree of homology with that of other eukaryotes, such as *Saccharomyces cerevisiae* (30.64%) (Figure 1), indicating that *CCTζ* is not conserved in the eukaryote.

SDS-PAGE results showed that there was an obvious band at about 29 kDa (Figure 2A). After ultrasonication, there was a clear protein band at 29 kDa in the ultrasonic precipitate, indicating that the *NbCCTζ*-233 was mainly expressed in the inclusion bodies. Ni-NTA purification results showed that the *NbCCTζ*-233 was well bound to the NTA column under denaturing conditions, and the target protein could be obtained by elution with 50 mM or 200 mM imidazole (Figure 2B). Western blot using preimmune serum as the negative control showed a specific band at about 57 kDa in the total proteins of *N. bombycis* (Figure 2C,D). These results indicate that the polyclonal antibody undergoes a specific antigen-antibody reaction.

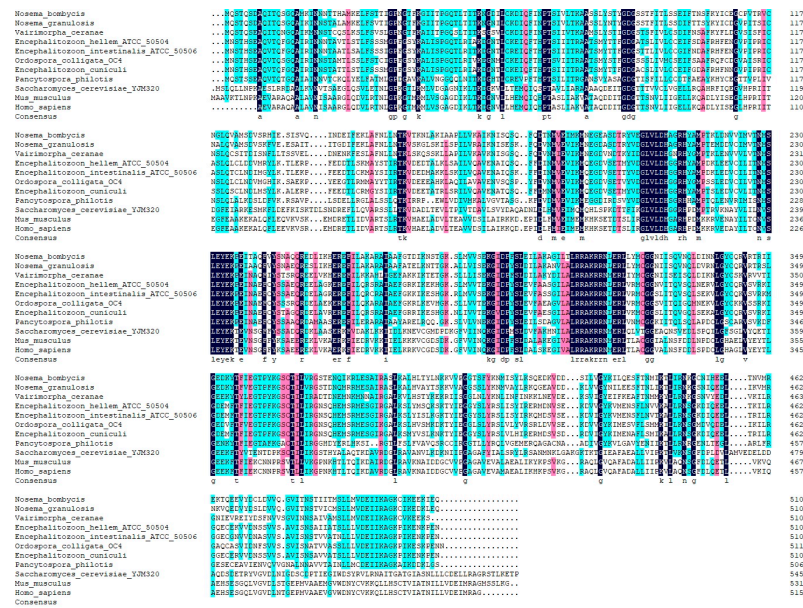


Figure 1. Multiple sequence alignment between CCTζ from *Nosema bombycis* and other eukaryotes.

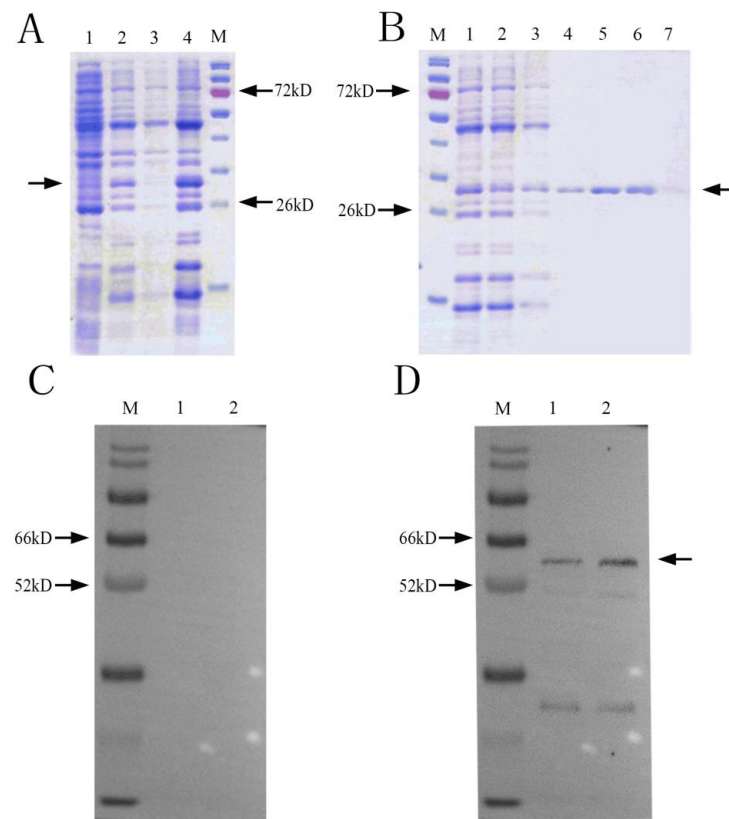
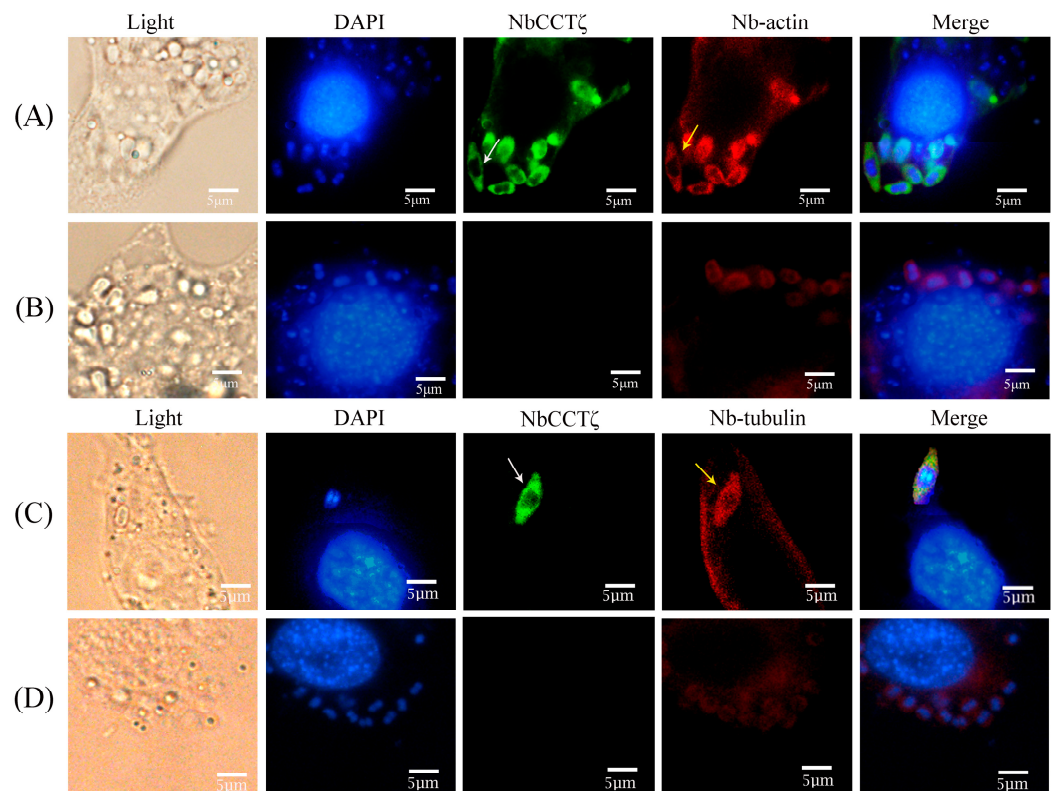


Figure 2. Recombinant protein expression and purification and Western blot analysis: (A) SDS-PAGE of expressed recombinant protein M: protein marker; 1: NbcCTζ-233 total cell lysate (uninduced); 2: NbcCTζ-233 total cell lysate (4 h after induction with 0.5 mM IPTG, 37 °C); 3: ultrasonic supernatant; 4: ultrasonic precipitation; Arrow indicates NbcCTζ-233 protein. (B) protein purification M: protein marker; 1: ultrasonic precipitation with urea solution (sample to be purified); 2: flowthrough; 3: 10 mM imidazole elution; 4: 20 mM imidazole elution; 5: 50 mM imidazole elution 6: 200 mM imidazole elution; 7: 500 mM imidazole elution; Arrow indicates NbcCTζ-233 protein (C) preimmune serum M: protein marker; 1 and 2: total protein of *N. bombycis*; (D) Western blot of NbcCTζ M: protein marker; 1 and 2: total protein of *N. bombycis*. Arrow indicates NbcCTζ protein.

### 3.2. Subcellular Localization of NbcCCT $\zeta$ in *N. bombycis*

An IFA (immunofluorescence assay) was performed to investigate the subcellular localization of NbcCCT $\zeta$  in the proliferative phase of *N. bombycis*. The NbcCCT $\zeta$  antibody was coupled with Alexa Fluor 488 (green), while the Nb-actin antibody or the Nb $\beta$ -tubulin antibody was coupled with Cy5 (red), and the nucleus was stained with DAPI (blue). IFA results show that the NbcCCT $\zeta$  genes are mainly distributed in the cytoplasm and completely overlap with Nb-actin (Figure 3A) or Nb $\beta$ -tubulin (Figure 3C) during the proliferative phase.



**Figure 3.** Colocalization analysis of NbcCCT $\zeta$  with Nb-actin and Nb $\beta$ -tubulin in the proliferative phase of *N. bombycis*: (A,C) proliferative phase; (B,D) preimmune serum. The white arrow indicates NbcCCT $\zeta$ ; the yellow arrow indicates the Nb-actin or Nb $\beta$ -tubulin. The white arrows indicated the green fluorescent signals (NbcCCT $\zeta$ ) and the yellow arrows indicated the red fluorescent signals (Nb-actin or Nb $\beta$ -tubulin).

### 3.3. NbcCCT $\zeta$ Interacts with NbcCCT $\alpha$ in Yeast Two-Hybrid Assay

The yeast with NbcCCT $\alpha$ -PGBKT7 and NbcCCT $\zeta$ -PGADT7 plasmids (Figure 4E) and the positive control (Figure 4B) strains with pGBKT7-p53 and pGADT7-T plasmids could still grow in a four-deficient medium (SD/-Leu/-Trp/-His/-Ade), while the negative control strains with pGBKT7-lam and pGADT7-T (Figure 4A) could not grow on this medium, indicating that NbcCCT $\zeta$  has a strong interaction with NbcCCT $\alpha$ .

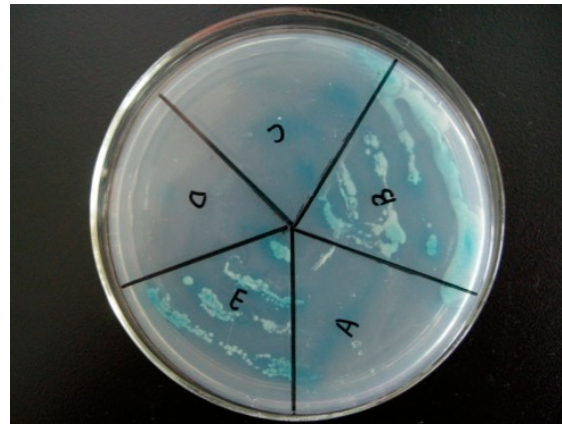


**Figure 4.** Validation of yeast two-hybrid positive plasmids: (A) negative control (pGBKT7-lam and pGADT7-T); (B) positive control (pGBKT7-p53 and pGADT7-T); (C) pGADT7 and pGBKT7-NbCCT $\alpha$ ; (D) pGBKT7 and pGADT7-NbCCT $\zeta$ ; (E) pGBKT7-NbCCT $\alpha$  and pGADT7-NbCCT $\zeta$ .

### 3.4. Colocalization of NbCCT $\zeta$ and NbCCT $\alpha$

To investigate the colocalization of NbCCT $\zeta$  with other subunits in the intracellular phase of *N. bombycis*, NbCCT $\alpha$  and NbCCT $\zeta$  were selected for colocalization using the IFA. NbCCT $\alpha$  and NbCCT $\zeta$  are labeled with green fluorescence and red fluorescence, respectively. In sporoplasm, NbCCT $\alpha$  and NbCCT $\zeta$  were distributed in the whole cell (Figure 5A). In the proliferative phase (Figure 5B) and the sporogenic phase (Figure 5C), NbCCT $\alpha$  and NbCCT $\zeta$  were mainly distributed in the cytoplasm. These results indicate that the NbCCT $\alpha$  and NbCCT $\zeta$  are colocalized throughout the entire life cycle of *N. bombycis*.

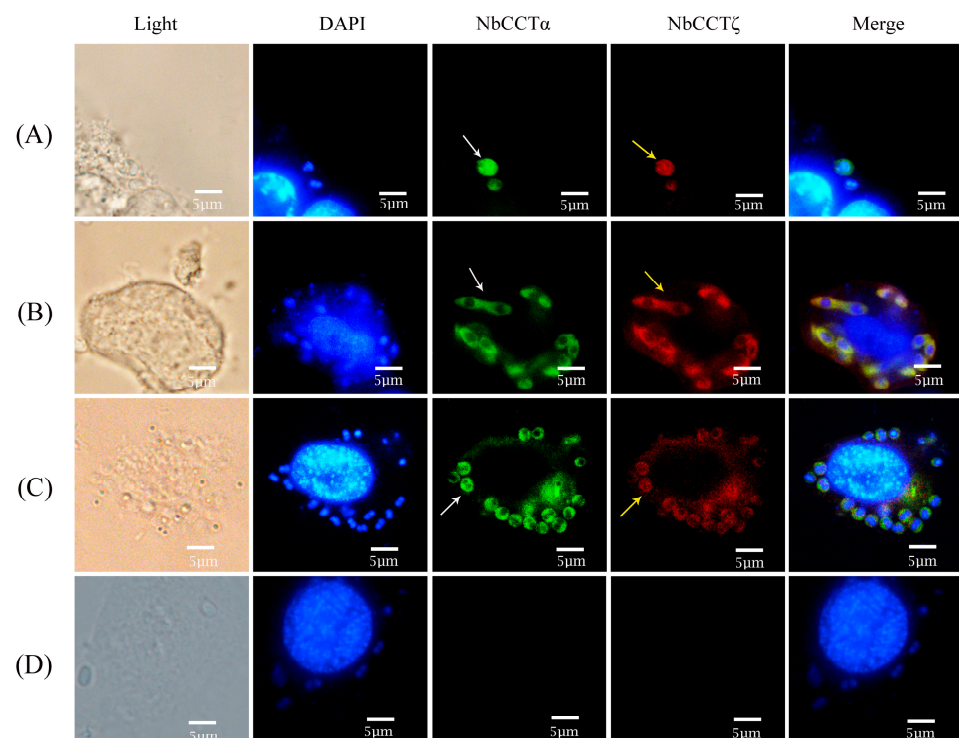


**Figure 5.** Colocalization analysis of NbCCT $\zeta$  and NbCCT $\alpha$  in the intracellular stage of *N. bombycis*: (A) sporoplasm; (B) meront; (C) sporoblast; (D) negative control. The white arrows indicated the green fluorescent signals (NbCCT $\zeta$ ) and the yellow arrows indicated the red fluorescent signals (NbCCT $\alpha$ ).

### 3.5. Knockdown of *NbCCTα* Downregulated the Expression of *NbCCTζ*, and the Knockdown of *NbCCTζ* Downregulated the Expression of *NbCCTα*

Our previous work has proved that RNAi can downregulate the expression of *NbCCTα* [24]. In this study, after the knockdown of *NbCCTα* or *NbCCTζ*, the relative expression of *NbCCTζ* or *NbCCTα* was detected by RT-qPCR using *NbssrRNA* as a reference gene. The transcriptional level of the *NbCCTζ* gene was extremely significantly downregulated at 24 h, 48 h, 72 h, and 96 h by the RNAi of *NbCCTα* (Figure 6A). After the RNAi of *NbCCTζ*, the transcriptional level of *NbCCTζ* was significantly downregulated at 24 h and 48 h (Figure 6B), while the transcriptional level of *NbCCTα* was extremely significantly downregulated at 24 h, 72 h, and 96 h (Figure 6C). These results indicate that *NbCCTζ* may functionally cooperate with *NbCCTα*.

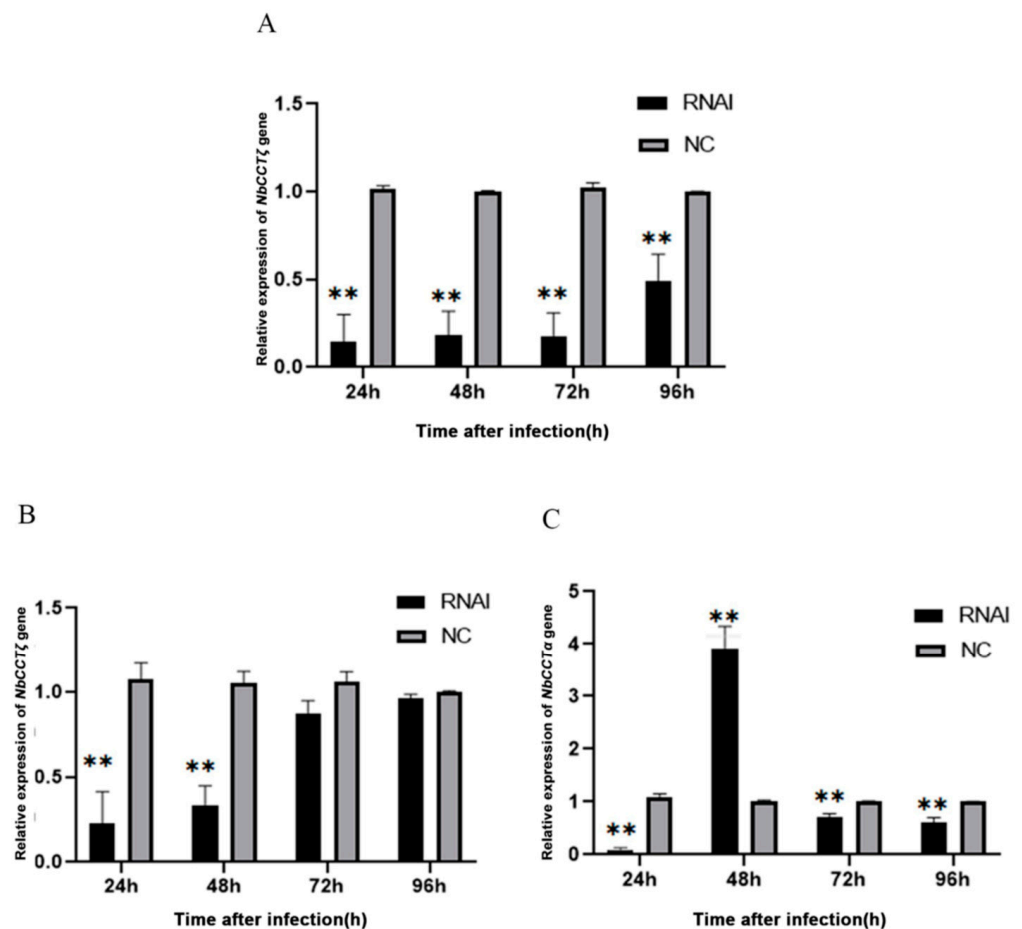


**Figure 6.** Transcriptional level of *NbCCTζ* and *NbCCTα* after RNAi: (A) the relative expression of the *NbCCTζ* gene after RNAi of *NbCCTα*. Error bars represent the standard deviation of three independent replicates ( $n = 3$ , mean  $\pm$  SE, \*\*  $p < 0.01$ ); (B) the relative expression of the *NbCCTζ* gene after RNAi of *NbCCTζ*. Error bars represent the standard deviation of three independent replicates ( $n = 3$ , mean  $\pm$  SE, \*\*  $p < 0.01$ ); (C) the relative expression of the *NbCCTα* gene after the RNAi of *NbCCTζ*. Error bars represent the standard deviation of three independent replicates ( $n = 3$ , mean  $\pm$  SE, \*\*  $p < 0.01$ ).

### 3.6. Knocking down *NbCCTζ* Suppressed the Proliferation of *N. bombycis*

The relative expression of the *NbCCTζ* gene was detected at all time points after infection and exhibited a gradual decline during the lifecycle of *N. bombycis* (Figure S2). To explore the effect of knocking down the *NbCCTζ* gene on the proliferation of *N. bombycis*, the transcriptional level of *NbssrRNA* was determined, which reflected the proliferation of *N. bombycis*. The effect of RNAi was analyzed by qPCR using *BmGAPDH* (glyceraldehyde-

3-phosphate dehydrogenase of *Bombyx mori*) as a reference gene. The transcriptional level of *NbssrRNA* was significantly downregulated by the RNAi of *NbCCTζ* at 24 h, 48 h, 72 h, and 96 h post-infection (Figure 7). These results suggest that *NbCCTζ* plays an important role in the proliferation of *N. bombycis*.

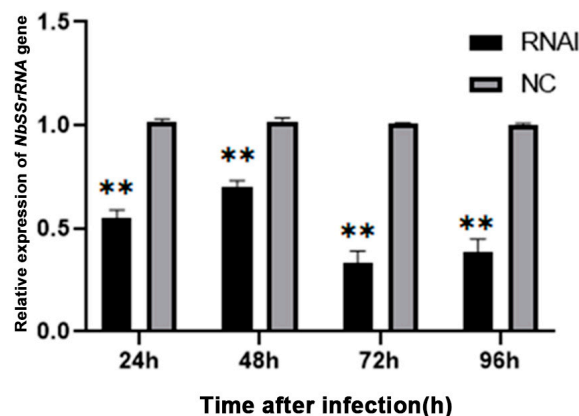


**Figure 7.** Relative expression of *NbssrRNA* gene after RNAi of *NbCCTζ*. Error bars represent the standard deviation of three independent replicates ( $n = 3$ , mean  $\pm$  SE, \*\*  $p < 0.01$ ).

#### 4. Discussion

CCT complexes are a class of molecular chaperones with highly homologous sequences and are involved in many basic cellular processes in organisms; they were first discovered in mouse spermatogonia by Silver [25]. They also help proteins properly fold, maintain protein conformation, and are critical for cell survival and growth [26]. Microsporidia have reduced numbers of chaperone proteins outside the CCT [27]; however, to date, no CCT complex has been found in microsporidia using cryo-EM [28,29].

Some CCT subunits, such as  $CCT\alpha$ ,  $CCT\gamma$ , and  $CCT\zeta$ , play an important role in the function of microtubule-associated proteins [30]. The C-terminal region of tubulin interacts with  $CCT\zeta$  [31]. In this study, our findings demonstrated that the *NbCCTζ* gene exhibited limited homology with eukaryotic counterparts while displaying a certain degree of similarity to other microsporidia. Nakjang S et al. found that the proteins that are conserved across all microsporidian genomes are likely to be particularly important for the maintenance of their parasitic lifestyle [32]. Our IFA results show that the *NbCCTζ* is mainly distributed in the cytoplasm and is colocalized with *Nb-actin* and *Nbβ-tubulin* in the proliferative phase. During the proliferative phase, the cytoskeletal proteins such as actin and tubulin are actively synthesized to enable cell division, as well as the intracellular transport of the components of the spore wall that starts forming at this stage [33]. These lines of evidence are similar to our previous findings on *NbCCTα* [24] and indicate that *NbCCTζ* may have a function like *NbCCTα* in the folding of tubulin and actin.

CCT consists of two heterogeneous eight-membered rings stacked back to back, forming a structure that encloses a folding cavity [5]. However, the arrangement of CCT subunits may be different in eukaryotes [34,35], and CCT subunits do not always assemble into a single form of hetero-oligomeric complex; instead, they confer independent functions in the cell [36]. Cong Y et al. reported that  $CCT\zeta$  interacts with  $CCT\alpha$  in the 4.0-Å single-particle cryo-EM-derived structure of bovine testis CCT [34]. The present study shows that *NbCCTζ* interacts with *NbCCTα*, and *NbCCTζ* is colocalized with *NbCCTα* throughout the entire life cycle of *N. bombycis*. The transcriptional level of *NbCCTζ* was significantly downregulated by knocking down the *NbCCTα* gene. The transcriptional level of *NbCCTα* was downregulated after the knockdown of the *NbCCTζ* gene at 24 h, 72 h, and 96 h, whereas it was significantly upregulated at 48 h; moreover, the proliferation of *N. bombycis* was significantly inhibited, indicating that the *NbCCTζ* plays a crucial role in the proliferation of *N. bombycis*. Our previous studies have revealed that *NbCCTα* is related to cell division, and *NbCCTδ* plays an efficient role in keeping the integrity of the

cytoskeleton [24,37]. Combining the results of this study with those of our previous work, we summarize our knowledge of the expression pattern and subcellular localization of CCT $\zeta$ , CCT $\delta$ , and CCT $\alpha$  in *N. bombycis* in Table S1, which may help to perform further research on the function and relationship of CCT subunits in microsporidia. Taken together, these lines of evidence suggest that the subunits of CCT not only perform independent functions but also cooperate to assist the modification of protein.

**Supplementary Materials:** The following supporting information can be downloaded at: <https://www.mdpi.com/article/10.3390/jof10030229/s1>, Figure S1: The PCR amplification of *NbCCT $\zeta$*  gene. Lane1: PCR amplification of *NbCCT $\zeta$*  gene; LaneM: DL2000 DNA ladder; Figure S2: The relative expression level of *NbCCT $\zeta$*  of *N. bombycis*. The *NbCCT $\zeta$*  expression levels at 96 h post-infection were used as reference. Error bars represent standard deviation of three independent replicates ( $n = 3$ , mean  $\pm$  SE); Table S1: The summary of the expression pattern and subcellular localization of CCT $\zeta$ , CCT $\delta$  and CCT $\alpha$ .

**Author Contributions:** Conceptualization, Z.S. and S.X.; methodology, S.X., Y.C., J.Q. and Z.S.; software, Q.W., Y.Z. and X.T.; writing—original draft preparation, S.X., Y.C. and J.Q.; writing—review and editing, R.W. and E.W.; supervision, Z.S. All authors have read and agreed to the published version of the manuscript.

**Funding:** This work was funded by the China Agriculture Research System of MOF and MARA.

**Institutional Review Board Statement:** Not applicable.

**Informed Consent Statement:** Not applicable.

**Data Availability Statement:** Data are contained within the article and Supplementary Materials.

**Acknowledgments:** We are grateful to all who provided the means for us to access free software, which we have used and cited in this article. We would also like to thank all partners and laboratory staff for their kind help and criticism.

**Conflicts of Interest:** The authors declare no conflicts of interest.

## References

- Guo, R.; Cao, G.; Lu, Y.; Xue, R.; Kumar, D.; Hu, X.; Gong, C. Exogenous gene can be integrated into *Nosema bombycis* genome by mediating with a non-transposon vector. *Parasitol. Res.* **2016**, *115*, 3093–3098. [CrossRef] [PubMed]
- Pan, G.; Xu, J.; Li, T.; Xia, Q.; Liu, S.-L.; Zhang, G.; Li, S.; Li, C.; Liu, H.; Yang, L.; et al. Comparative genomics of parasitic silkworm microsporidia reveal an association between genome expansion and host adaptation. *BMC Genom.* **2013**, *14*, 186. [CrossRef] [PubMed]
- Li, Z.; Wang, Y.; Wang, L.; Zhou, Z. Molecular and biochemical responses in the midgut of the silkworm, *Bombyx mori*, infected with *Nosema bombycis*. *Parasites Vectors* **2018**, *11*, 147. [CrossRef] [PubMed]
- Gao, Y.; Thomas, J.O.; Chow, R.L.; Lee, G.H.; Cowan, N.J. A cytoplasmic chaperonin that catalyzes beta-actin folding. *Cell* **1992**, *69*, 1043–1050. [CrossRef]
- Leitner, A.; Joachimiak, L.A.; Bracher, A.; Mönkemeyer, L.; Walzthoeni, T.; Chen, B.; Pechmann, S.; Holmes, S.; Cong, Y.; Ma, B.; et al. The molecular architecture of the eukaryotic chaperonin TRiC/CCT. *Structure* **2012**, *20*, 814–825. [CrossRef]
- Llorca, O.; Martín-Benito, J.; Gómez-Puertas, P.; Ritco-Vonsovici, M.; Willison, K.R.; Carrascosa, J.L.; Valpuesta, J.M. Analysis of the Interaction between the Eukaryotic Chaperonin CCT and Its Substrates Actin and Tubulin. *J. Struct. Biol.* **2001**, *135*, 205–218. [CrossRef]
- Hein, M.Y.; Hubner, N.C.; Poser, I.; Cox, J.; Nagaraj, N.; Toyoda, Y.; Gak, I.A.; Weisswange, I.; Mansfeld, J.; Buchholz, F.; et al. A human interactome in three quantitative dimensions organized by stoichiometries and abundances. *Cell* **2015**, *163*, 712–723. [CrossRef]
- Trinidad, A.G.; Muller, P.A.; Cuellar, J.; Klejnot, M.; Nobis, M.; Valpuesta, J.M.; Vousden, K.H. Interaction of p53 with the CCT complex promotes protein folding and Wild-Type p53 activity. *Mol. Cell* **2013**, *50*, 805–817. [CrossRef]
- Willison, K.R. The substrate specificity of eukaryotic cytosolic chaperonin CCT. *Philos. Trans. R. Soc. B Biol. Sci.* **2018**, *373*, 20170192. [CrossRef] [PubMed]
- Grantham, J.; Brackley, K.I.; Willison, K.R. Substantial CCT activity is required for cell cycle progression and cytoskeletal organization in mammalian cells. *Exp. Cell Res.* **2006**, *312*, 2309–2324. [CrossRef] [PubMed]
- Wei, Q.; Zhu, G.; Cui, X.; Kang, L.; Cao, D.; Jiang, Y. Expression of CCT6A mRNA in chicken granulosa cells is regulated by progesterone. *Gen. Comp. Endocrinol.* **2013**, *189*, 15–23. [CrossRef]

12. Génier, S.; Degrandmaison, J.; Moreau, P.; Labrecque, P.; Hébert, T.E.; Parent, J.-L. Regulation of GPCR expression through an interaction with CCT7, a subunit of the CCT/TRiC complex. *Mol. Biol. Cell* **2016**, *27*, 3800–3812. [[CrossRef](#)] [[PubMed](#)]
13. Kubota, H. Function and regulation of cytosolic molecular chaperone CCT. *Vitam. Horm.* **2002**, *65*, 313–331. [[PubMed](#)]
14. Yébenes, H.; Mesa, P.; Muñoz, I.G.; Montoya, G.; Valpuesta, J.M. Chaperonins: Two rings for folding. *Trends Biochem. Sci.* **2011**, *36*, 424–432. [[CrossRef](#)] [[PubMed](#)]
15. Showalter, A.E.; Martini, A.C.; Nierenberg, D.; Hosang, K.; Fahmi, N.A.; Gopalan, P.; Khaled, A.S.; Zhang, W.; Khaled, A.R. Investigating Chaperonin-Containing TCP-1 subunit 2 as an essential component of the chaperonin complex for tumorigenesis. *Sci. Rep.* **2020**, *10*, 798. [[CrossRef](#)] [[PubMed](#)]
16. Yang, X.; Ren, H.; Shao, Y.; Sun, Y.; Zhang, L.; Li, H.; Zhang, X.; Yang, X.; Yu, W.; Fu, J. Chaperonin-containing T-complex protein 1 subunit 8 promotes cell migration and invasion in human esophageal squamous cell carcinoma by regulating  $\alpha$ -actin and  $\beta$ -tubulin expression. *Int. J. Oncol.* **2018**, *52*, 2021–2030. [[CrossRef](#)]
17. Yin, H.; Miao, X.; Wu, Y.; Wei, Y.; Zong, G.; Yang, S.; Chen, X.; Zheng, G.; Zhu, X.; Guo, Y.; et al. The role of the Chaperonin containing t-complex polypeptide 1, subunit 8 (CCT8) in B-cell non-Hodgkin's lymphoma. *Leuk. Res.* **2016**, *45*, 59–67. [[CrossRef](#)]
18. Dou, L.; Zhang, X. Upregulation of CCT3 promotes cervical cancer progression through FN1. *Mol. Med. Rep.* **2021**, *24*, 856. [[CrossRef](#)]
19. Wang, Y.; Liu, P.; Zhang, Z.; Wang, J.; Cheng, Z.; Fan, C. Identification of CCT3 as a prognostic factor and correlates with cell survival and invasion of head and neck squamous cell carcinoma. *Biosci. Rep.* **2021**, *41*, BSR20211137. [[CrossRef](#)]
20. Yam, A.Y.; Xia, Y.; Lin, H.-T.J.; Burlingame, A.; Gerstein, M.; Frydman, J. Defining the TRiC/CCT interactome links chaperonin function to stabilization of newly made proteins with complex topologies. *Nat. Struct. Mol. Biol.* **2008**, *15*, 1255–1262. [[CrossRef](#)]
21. Van Hove, I.; Verslegers, M.; Hu, T.; Carden, M.; Arckens, L.; Moons, L. A proteomic approach to understand MMP-3-driven developmental processes in the postnatal cerebellum: Chaperonin CCT6A and MAP kinase as contributing factors. *Dev. Neurobiol.* **2015**, *75*, 1033–1048. [[CrossRef](#)]
22. Wang, R.; Chen, Y.; Xu, S.; Wei, E.; He, P.; Wang, Q.; Zhang, Y.; Tang, X.; Shen, Z. Ssn6 Interacts with Polar Tube Protein 2 and Transcriptional Repressor for RNA Polymerase II: Insight into Its Involvement in the Biological Process of Microsporidium *Nosema bombycis*. *J. Fungi* **2023**, *9*, 990. [[CrossRef](#)]
23. Sun, F.; Wang, R.; He, P.; Wei, E.; Wang, Q.; Tang, X.; Zhang, Y.; Zhu, F.; Shen, Z. Sar1 Interacts with Sec23/Sec24 and Sec13/Sec31 Complexes: Insight into Its Involvement in the Assembly of Coat Protein Complex II in the Microsporidian *Nosema bombycis*. *Microbiol. Spectr.* **2022**, *10*, e0071922. [[CrossRef](#)] [[PubMed](#)]
24. Yao, M.; Wang, R.; Chen, Y.; He, P.; Wei, E.; Zhu, F.; Wang, Q.; Zhang, Y.; Tang, X.; Shen, Z. Identification and subcellular localization analysis of CCT $\alpha$  in microsporidian *Nosema bombycis*. *Infect. Genet. Evol.* **2022**, *102*, 105309. [[CrossRef](#)]
25. Silver, L.M.; Artzt, K.; Bennett, D. A major testicular cell protein specified by a mouse T/t complex gene. *Cell* **1979**, *17*, 275–284. [[CrossRef](#)]
26. Hartl, F.U.; Bracher, A.; Hayer-Hartl, M. Molecular chaperones in protein folding and proteostasis. *Nature* **2011**, *475*, 324–332. [[CrossRef](#)] [[PubMed](#)]
27. Heinz, E.; Williams, T.A.; Nakjang, S.; Noël, C.J.; Swan, D.C.; Goldberg, A.V.; Harris, S.R.; Weinmaier, T.; Markert, S.; Becher, D.; et al. The genome of the obligate intracellular parasite *Trachipleistophora hominis*: New insights into microsporidian genome dynamics and reductive evolution. *PLoS Pathog.* **2012**, *8*, e1002979. [[CrossRef](#)]
28. Barandun, J.; Hunziker, M.; Vossbrinck, C.R.; Klinge, S. Evolutionary compaction and adaptation visualized by the structure of the dormant microsporidian ribosome. *Nat. Microbiol.* **2019**, *4*, 1798–1804. [[CrossRef](#)] [[PubMed](#)]
29. Jespersen, N.; Ehrenbolger, K.; Winiger, R.R.; Svedberg, D.; Vossbrinck, C.R.; Barandun, J. Structure of the reduced microsporidian proteasome bound by PI31-like peptides in dormant spores. *Nat. Commun.* **2022**, *13*, 6962. [[CrossRef](#)]
30. Roobol, A.; Sahyoun, Z.P.; Carden, M.J. Selected subunits of the cytosolic chaperonin associate with microtubules assembled in vitro. *J. Biol. Chem.* **1999**, *274*, 2408–2415. [[CrossRef](#)]
31. Leroux, M.R.; Hartl, F. Protein folding: Versatility of the cytosolic chaperonin TRiC/CCT. *Curr. Biol.* **2000**, *10*, R260–R264. [[CrossRef](#)] [[PubMed](#)]
32. Nakjang, S.; Williams, T.A.; Heinz, E.; Watson, A.K.; Foster, P.G.; Sendra, K.M.; Heaps, S.E.; Hirt, R.P.; Embley, T.M. Reduction and expansion in microsporidian genome evolution: New insights from comparative genomics. *Genome Biol. Evol.* **2013**, *5*, 2285–2303. [[CrossRef](#)] [[PubMed](#)]
33. Cali, A.; Takvorian, P.M. Developmental morphology and life cycles of the microsporidia. In *Microsporidia: Pathogens of Opportunity*; John Wiley & Sons, Inc.: Hoboken, NJ, USA, 2014; pp. 71–133.
34. Cong, Y.; Baker, M.L.; Jakana, J.; Woolford, D.; Miller, E.J.; Reissmann, S.; Kumar, R.N.; Redding-Johanson, A.M.; Batth, T.S.; Mukhopadhyay, A.; et al. 4.0-Å resolution cryo-EM structure of the mammalian chaperonin TRiC/CCT reveals its unique subunit arrangement. *Proc. Natl. Acad. Sci. USA* **2010**, *107*, 4967–4972. [[CrossRef](#)] [[PubMed](#)]
35. Dekker, C.; Roe, S.M.; McCormack, E.A.; Beuron, F.; Pearl, L.H.; Willison, K.R. The crystal structure of yeast CCT reveals intrinsic asymmetry of eukaryotic cytosolic chaperonins. *EMBO J.* **2011**, *30*, 3078–3090. [[CrossRef](#)]

36. Wagner, C.T.; Lu, I.Y.; Hoffman, M.H.; Sun, W.Q.; Trent, J.D.; Connor, J. T-complex Polypeptide-1 interacts with the erythrocyte cytoskeleton in response to elevated temperatures. *J. Biol. Chem.* **2004**, *279*, 16223–16228. [[CrossRef](#)]
37. Qi, J.; Zhu, F.; Shao, L.; Chen, Y.; Li, J.; He, P.; Shang, R.; Sun, F.; Wang, Q.; Zhang, Y.; et al. CCT $\delta$  colocalizes with actin and  $\beta$ -tubulin: Insight into its involvement in the cytoskeleton formation of the intracellular parasite *Nosema bombycis*. *J. Invertebr. Pathol.* **2021**, *184*, 107646. [[CrossRef](#)]

**Disclaimer/Publisher's Note:** The statements, opinions and data contained in all publications are solely those of the individual author(s) and contributor(s) and not of MDPI and/or the editor(s). MDPI and/or the editor(s) disclaim responsibility for any injury to people or property resulting from any ideas, methods, instructions or products referred to in the content.